



HAL
open science

Aptamer-modified pencil graphite electrodes for the impedimetric determination of ochratoxin A

Gültekin Gökçe, Sondes Ben Aissa, Katarína Nemčková, Nouredine Raouafi, Jean-Louis Marty, Gaëlle Catanante

► **To cite this version:**

Gültekin Gökçe, Sondes Ben Aissa, Katarína Nemčková, Nouredine Raouafi, Jean-Louis Marty, et al.. Aptamer-modified pencil graphite electrodes for the impedimetric determination of ochratoxin A. Food Control, 2020, 115, pp.107271. 10.1016/j.foodcont.2020.107271 . hal-03945517

HAL Id: hal-03945517

<https://hal.science/hal-03945517v1>

Submitted on 23 Aug 2024

HAL is a multi-disciplinary open access archive for the deposit and dissemination of scientific research documents, whether they are published or not. The documents may come from teaching and research institutions in France or abroad, or from public or private research centers.

L'archive ouverte pluridisciplinaire **HAL**, est destinée au dépôt et à la diffusion de documents scientifiques de niveau recherche, publiés ou non, émanant des établissements d'enseignement et de recherche français ou étrangers, des laboratoires publics ou privés.

Aptamer-modified Pencil graphite electrodes for the impedimetric determination of ochratoxin A

Gültekin Gökçe^{a, b, *}, Sondes Ben Aissa^{a, c}, Katarína Nemčeková^{a, d}, Gaëlle Catanante^a,
Noureddine Raouafi^c and Jean-Louis Marty^{a, *}

^a Université de Perpignan Via Domitia, BAE-LBBM: Biocapteurs-Analyses-Environment, 66860 Perpignan CEDEX, France

^b Cumhuriyet University, Pharmacy Faculty, 58140 Sivas, Turkey

^c Université de Tunis El Manar, Faculté des Sciences de Tunis, Laboratoire de Chimie Analytique et Electrochimie, Sensors and Biosensors Group, Campus Universitaire de Tunis El Manar, 2092 Tunis, Tunisia

^d Slovak University of Technology in Bratislava, Faculty of Chemical and Food Technology, Institute of Analytical Chemistry, 812 37 Bratislava, Slovakia (katarina.nemcekova@stuba.sk)

* Corresponding authors: ggokce2000@gmail.com/ +905056299497 and
jlmarty@univ-perp.fr / +33 4 68 66 22 54

1 **Abstract**

2 Ochratoxin A (OTA), a widespread food contaminant, is considered as one of the most
3 hazardous mycotoxins commonly occurring in beer. Herein, we describe a novel impedimetric
4 aptasensor based on Pencil Graphite Electrodes (PGE) for the analysis of OTA. Taking
5 advantage of its affordability and high active surface area, a PGE was modified with a
6 specific aptamer, to achieve sensitive detection of OTA. This strategy relies on the target-
7 induced increase in the electron transfer resistance (R_{ct}) upon OTA recognition using
8 ferro/ferricyanide as a redox probe. With the addition of OTA, the formation of OTA–aptamer
9 complex resulted in an increase of R_{ct} . The change of R_{ct} strongly depends on OTA
10 concentration, which is applied for mycotoxin quantification. An acceptable linear range was
11 obtained from 0.1 to 2.0 ng.mL⁻¹ with a very good limit of detection as low as 0,1 ng.mL⁻¹.
12 This simple-to-design aptasensor was successfully tested in spiked beer samples, with OTA
13 concentrations in the range of 0.4-1.6 ng.mL⁻¹, attesting a recovery percentage of 93.4 ± 6.6%.
14 It also showed a high level of stability and reproducibility thanks to the electro-grafting
15 method via in-situ generation of 4-carboxyphenyl diazonium salts. This PGE-based platform
16 is a versatile approach for the design of low-cost aptasensors for food safety control.

17 **Keywords**

18 Electrochemical Aptasensor, Pencil Graphite Electrode, Electrochemical Impedance
19 Spectroscopy, Diazonium Electrografting, Ochratoxin A.

20

21 1. Introduction

22 In order to improve human life, the progresses in technologies as well as the mass industrial
23 production of novel materials have rapidly become a part of everyday life. As a consequence,
24 various global health risks including the increase of pollutants and toxins in food industry
25 have occurred (Nácher-Mestre *et al.*, 2015). For these reasons, a food contamination has been
26 getting more attention and, nowadays, it represents one of the most important worldwide
27 issues. The food commodities are often exposed to a variety of mycotoxins which are
28 produced at inconvenient conditions, such as air humidity and regulation, temperature, time of
29 storage etc. OTA belongs to the class of the most toxic species of mycotoxins which is
30 produced by several fungi, such as *Penicillium verrucosum* and by several species of
31 *Aspergillus* (Bui-Klimke & Wu, 2015).

32 The relatively high levels of OTA concentration are principally found in cereals, grape juice,
33 coffee, nuts, spices, cocoa beans or wine. Because of the chemical stability of OTA and its
34 long half-life in mammalian tissues, the contamination could be also occurred in pork and pig
35 blood products as well as in beer beverages (Walker, 2002). Since almost all countries did not
36 provide information on the contribution of food products, the overall intake values from
37 OTA-contaminated food commodities were calculated, whereby cereals resulted as the main
38 contributors (50%) followed by wine (13%), coffee (10%), spices (8%), others (6%), beer
39 (5%), cocoa (4%), dried fruits (3%) and meat (1%) (Europea, 2002). According to The
40 International Agency for Research on Cancer (IARC) (IARC, 1994) and The World Health
41 Organization (WHO, 2007), OTA has been shown to be nephrotoxic, carcinogenic,
42 teratogenic and immunotoxic to human and animal beings and causes kidney and liver
43 tumors. The consumption of OTA-contaminated foods has a huge negative impact on
44 population health hand must be controlled. The maximum levels of OTA concentration in a
45 wide range of foodstuffs available in European countries have been established in 2002 by the
46 Directorate-General Health and Consumer Protection (SANCO), responsible for EU
47 legislation in the areas of food safety, safety of products, public health and consumer safety.

48 As beer products play an important role in social life, their consumption has reached to
49 significantly high levels. For this reason, the continual control of OTA concentration in beer
50 products is required. According to SANCO, the daily dietary intakes of OTA ranges from
51 0,01 ng/kg (Italy) to 0,14 ng/kg (Denmark) (Europea, 2002). The most commonly used
52 analytical approaches for OTA detection are liquid chromatography (LC) with fluorescence

53 detectors (Appell *et al.*, 2018), gas chromatography with mass spectrometry (GC-MS)
54 (Olsson *et al.*, 2002), thin layer chromatography (TLC) (Patterson & Roberts, 1979), or
55 enzyme linked immunosorbent assay (ELISA) (Flajs *et al.*, 2009). However, electrochemical
56 biosensors (EBs) represent appealing analytical tools, owing a good price/performance ratio
57 and providing a relatively fast detection of target analyte, which make them great candidates
58 for mycotoxins detection in food samples. Generally, these EBs consist of an ingenious
59 combination of bioreceptor and signal transducer. Among different biorecognition elements
60 (including enzymes, amino acids, nucleic acids, tissues, cells, etc.), aptamers are emerging
61 synthetic biomolecules originated from in vitro selection (SELEX) (Blind & Blank, 2015) that
62 offer several advantages in biomolecular recognition, including their high thermal and
63 chemical stability, great affinity and specificity for a wide range of targets, and low-cost
64 production (Labuda *et al.*, 2010). Aptamers are able to undergo a unique three-dimensional
65 structure upon binding to target which provides a great flexibility during the development of
66 aptamer-based EBs or E-aptasensors. They are often tagged with a redox label, such as
67 methylene blue (Guo *et al.*, 2015) or ferrocene (Ferapontova *et al.*, 2008) in order to perform
68 the electrochemical detection of analyte based on the measurement of a current signal
69 generated from the oxidation/reduction of the redox label at a fixed/variable potential. The
70 change in the current corresponds to the concentration of the analyte in the sample. On the
71 other hand, the conformational changes of an aptamer sequence need to be performed in a
72 relatively large area which ends in increasing the distance of the electro-active label from the
73 transducer surface. Moreover, the process of aptamer labeling is quite expensive and the
74 construction strategies of analysis are more complex and time-consuming because the labeling
75 can decrease the activity of immobilized biomolecules (Daniels & Pourmand, 2007; Rhouati
76 *et al.*, 2016). A better alternative may be to develop a label-free impedimetric aptasensor
77 using the electrochemical impedance spectroscopy (EIS) as a detection technique. Heretofore,
78 the EIS has become the most reported transduction approach because it allows performing a
79 direct sensitive detection of target analyte via monitoring the interfacial reaction mechanisms
80 and the dynamics of biomolecular interactions. Therefore, many impedimetric aptasensors
81 have been developed to successfully detect a variety of mycotoxins in food samples (Chen *et al.*
82 *et al.*, 2015; Danesh *et al.*, 2018; Khan *et al.*, 2019; Mishra *et al.*, 2015; Ocaña & del Valle,
83 2018).

84 On the other hand, cheap pencil mines, commonly named Pencil Graphite Electrode (PGE),
85 have been increasingly investigated as working electrodes for biosensing applications. These

86 available carbonaceous transducers show a great potential in developing EBs ensuring a
87 reliable option in disposable biosensors (Torrinha *et al.*, 2018). Recent reviews evidenced that
88 PGE paved the way to be considered as valuable alternative to other carbon-based electrodes
89 thanks to their thin dimensions and negligible cost (David *et al.*, 2017). However, as far we
90 know, a relevant part of published works refers to the immobilization of enzymes as
91 bioreceptors. The application of PGE with aptamers is still limited and even non-existing in
92 mycotoxins analysis field, predicting a new window of opportunities in research.

93 A crucial step throughout the development of electrochemical aptasensor is the optimization
94 of aptamer immobilization strategy. One of the simplest immobilization methods is the
95 physical adsorption of aptamer onto electrode surface via electrostatic interactions. However,
96 a poor reproducibility and sensitivity can be achieved. Moreover, the physical hindrance of
97 target analytes with a low molecular weight could be insufficient for observing the signal
98 variations. For these reasons, the activation of the electrode surface by desired functional
99 groups, according to their coupling partners, can be performed using various electro-grafting
100 methods (Bélanger & Pinson, 2011; Jiang *et al.*, 2017; Yáñez-Sedeño *et al.*, 2018).

101 This work describes the development of a label-free electrochemical impedimetric aptasensor,
102 based on PGEs for the rapid detection of OTA and its quantification in beer samples. Briefly,
103 the PGE surface was electrografted with 4-carboxyphenyl (4-CP) groups via *in-situ* generated
104 4-ABA diazonium salts in order to immobilize NH₂-modified anti-OTA aptamers via amide
105 coupling. The detection strategy is based on target-induced variation in charge transfer
106 resistance, which is measurable using electrochemical impedance spectroscopy. Analysis is
107 then performed by studying the change in electrical or physical properties of the PGE surface
108 which depend solely on the affinity of interaction between OTA and its specific aptamer and
109 thus the concentration of the mycotoxin in samples.

110

111 2. Experimental section

112 2.1 Reagents and materials

113 The amine modified aptamer of following sequence (Cruz-Aguado & Penner, 2008) was
114 purchased from Microsynth (Balgach, Switzerland):

115 NH₂-5'-GATCGGGTGTGGGTGGCGTAAAGGGAGCATCGGACA-3'.

116 Sodium phosphate dibasic (Na₂HPO₄), potassium phosphate monobasic (KH₂PO₄),
117 Magnesium chloride (MgCl₂), potassium chloride (KCl), sulfuric acid (H₂SO₄,98%), sodium
118 chloride (NaCl), hydrochloric acid (HCl, 37%), acetic acid (CH₃COOH, 98%) ethanol
119 (C₂H₆O, 98%), sodium nitrite (NaNO₂), *N*-hydroxysuccinimide (NHS), *N*-(3-
120 dimethylaminopropyl)-*N'*-ethylcarbodiimide hydrochloride (EDC), potassium ferrocyanide
121 (K₄[Fe(CN)₆]), potassium ferricyanide (K₃[Fe(CN)₆]), 4-aminobenzoic acid, and
122 ethanolamine (C₂H₇NO) were purchased from Sigma-Aldrich (Saint-Quentin-Fallavier,
123 France).

124 Aptamer solutions were prepared in binding buffer (BB, pH 7.4) containing 1 mM MgCl₂,
125 140 mM NaCl, 2.7 mM KCl, 0.1 mM Na₂HPO₄ and 1.8 mM KH₂PO₄. Acetate buffer solution
126 (ABS, 0,5 M) was used in the pretreatment of PGEs. All solutions were prepared in deionized
127 Milli- Q water (Millipore, Bedford, MA, USA). OTA purchased from Merck-sigma Aldrich
128 (Saint-Quentin-Fallavier, France) was firstly dissolved in methanol (5 mg. mL⁻¹) and
129 subsequently diluted in BB.

130 2.2 Apparatus

131 All measurements were performed using the electrochemical workstation SP-150 from Bio-
132 Logic Science Instruments (France), connected to the EC-Lab software V.11.25. A
133 conventional three-electrode system was used, consisting of Ag/AgCl reference, PGE as
134 working electrode ($\varphi=0.5$ mm) and platinum wire as counter electrode. The immersed contact
135 area of graphite working electrodes in all measurement solutions corresponds to 1.5 cm in
136 length. This specification is required to obtain reproducible results. In order to provide
137 electrical conductivity between disposable graphite lead and lead holder (pencil) a conductive
138 wire was soldered to the metallic part of the holder.

139 2.3 Design of the aptasensor

140 Before running the experiment, all the PGEs were uniformly cut to a 3 cm length then the
141 useful surface of 1,5 cm was immersed into the electrochemical cell solution for pretreatment.

142 In a first step, PGE transducers were pretreated in the acetate buffer solution (ABS, pH 4.8,
143 20 mM NaCl contained) by applying 1.40 V for 30 s without stirring. After that, reproducible
144 bare electrodes were carefully selected for further modifications, based on CV and EIS
145 measurements in 5 mM $[\text{Fe}(\text{CN})_6]^{3-/4-}$ solution.

146 Subsequently, the diazotation process was achieved by mixing 4-aminobenzoic acid (4-ABA)
147 diluted in 0.5 M HCl with 1.43-fold excess of sodium nitrite. The solution was left to react
148 for 10 minutes in a cooling bath for maximum generation of 4-carboxyphenyl (4-CP)
149 diazonium salt. Afterward, the electrodeposition was carried out via linear sweep voltammetry
150 (LSV) with potential ranging from 0.5 to -0.1 V and a scan rate of 50 $\text{mV}\cdot\text{s}^{-1}$. LS
151 voltammogram showed a cathodic peak of 4-CP diazonium salt at -0.2 V (See inset LSV
152 graph in Fig. 1). In this method, the electrochemical *in-situ* reduction of a diazonium salt
153 leads to the formation of aryl centered radicals after the spontaneous elimination of dinitrogen
154 gas (N_2). They form a robust covalent bond with the carbonaceous electrode surface by using
155 LSV (Khan *et al.*, 2019). This method allows to get a well-defined carboxyl-modified layer on
156 the electrode surface with a high level of stability and reproducibility (Yáñez-Sedeño *et al.*,
157 2018). The terminal COOH groups of 4-CP-functionalized PGE surface, were then activated
158 through EDC/NHS chemistry for the immobilization NH_2 -modified OTA aptamer via
159 covalent amide coupling, at an optimized concentration of $0.8\mu\text{M}$.

160 A schematic representation of the stepwise design strategy of the developed impedimetric
161 aptasensor is shown in Fig. 1. Such prepared aptasensors could be freshly used or stored at

Preferred place for Fig. 1

162 4°C for several days without significant loss of sensitivity and reproducibility of the PGE-
163 modified platform.

164 **2.4 Electrochemical measurements**

165 All the modification steps were characterized by cyclic voltammetry (CV) and
166 electrochemical impedance spectroscopy (EIS). The CV was carried out within potential
167 range of 0.0 V to 0.5 V and scan rate of 100 $\text{mV}\cdot\text{s}^{-1}$. The impedance spectra were recorded
168 using a sinusoidal AC potential perturbation of 5 mV (rms), in the frequency range from 10^5 -
169 10^{-1} Hz, superimposed on a DC potential of 0.1 V. All measurements were performed in a

170 solution of 5 mM ferri/ferrocyanide redox indicator $[\text{Fe}(\text{CN})_6]^{3-/4-}$ in BB, pH 7.4, as a
171 background electrolyte.

172 In this work, we focused on the variation in electron transfer resistance (R_{ct}) to quantify the
173 targeted mycotoxin in samples. In order to minimize the electrode to electrode variations and
174 to obtain reproducible and independent results, relative and normalized signals were required.
175 Accordingly, the ΔRatio parameter, subtracting the error due to inherent differences between
176 bare electrodes, was calculated for all the PGEs as following:

$$177 \quad \Delta\text{Ratio} = R_{\text{ct (after OTA)}} - R_{\text{ct (bare)}} / R_{\text{ct (before OTA)}} - R_{\text{ct (bare)}}$$

178 where $R_{\text{ct (after OTA)}}$ is the value obtained after incubation of OTA, $R_{\text{ct (bare)}}$ is the charge
179 transfer resistance of the bare electrode, and $R_{\text{ct (before OTA)}}$ is registered in blank BB before
180 OTA detection.

181 **2.5 Ochratoxin A aptasensing**

182 A stock solution of OTA was prepared in methanol (5 mg.mL^{-1}) and subsequently diluted in
183 binding buffer. For OTA aptasensing, selected concentrations ranging from 0.1 to 6.4 ng.mL^{-1}
184 ¹, including the maximum admissible level in beer samples of 2 ng.mL^{-1} , were tested. A small
185 standard solutions volume of $200 \mu\text{L}$ was required for modified-PGEs incubation. Based on
186 previous works published by our group ((Hayat et al., 2013), (Mishra et al., 2015)), an
187 incubation time of 1h was sufficient to enable the aptamer's structure to switch upon OTA
188 recognition. This time has been thus selected for OTA analysis. Afterward, the fabricated
189 PGEs were thoroughly rinsed with BB to carry out electrochemical measurements.

190 **2.6 Beer samples analysis**

191 A rapid and simple pretreatment is required before real sample analysis. The beer samples
192 were therefore prepared following a previously established protocol (Rhouati *et al.*, 2013).
193 Briefly, three samples were spiked with known concentrations of OTA stock solutions freshly
194 prepared in binding buffer. Then, all samples (spiked and blank) were cooled at 4°C for
195 30 min to prevent rapid foam formation, which may lead to sample overflow during the
196 degassing step. This latter step is performed by mean of an ultrasonic bath for up to 1 h. The
197 pH of prepared samples was then checked to be adjusted to 7.4 using BB if needed. Finally,
198 the prepared beer samples were filtered through a syringe filter of 0.45 μm to minimize

199 potential matrix interferences. After pretreatment, samples are directly tested following the
200 same protocol described for standard OTA solutions.

201 3. Results and discussion

202 3.1 Electrochemical characterization of the aptasensor

203 Electrochemical characterizations using CV and EIS were performed in the presence of

204 Preferred place for Fig. 2

204 $[\text{Fe}(\text{CN})_6]^{3-/4-}$ redox indicator in order to investigate the electrode surface properties as well as
205 to confirm the effectiveness of surface modification in each development step of the
206 aptasensor.

207 3.1.1. Cyclic voltammetry characterization

208 The electron transfer at the interface electrode-electrolyte was studied after each step of
209 surface modification and the CV results are presented in Fig. 2A. The sequential fabrication
210 of aptasensor was characterized by monitoring the changes in the current response of a redox
211 couple and the changes in the peak-to-peak separation. The electrochemical behavior of redox
212 indicator on PGE surface showed a characteristic reversible system with the cathodic/anodic
213 current peak ratio of approximately 1 and the peak-to-peak separation of 0.05 V.

214 The approximate specific surface area of bare PGE can be estimated according to Randles-
215 Sevcik formula, $I_p = 2.69 \times 10^5 D^{1/2} n^{3/2} A V^{1/2} C$ (where I_p is the redox peak current (A); n is
216 the electron transfer number, $n(\text{Fe}(\text{CN})_6^{3-/4-})=1$; C is the concentration of $\text{Fe}(\text{CN})_6^{3-/4-}$)
217 ($\text{mol} \cdot \text{cm}^{-3}$); A is the surface area (cm^2); D is the diffusion coefficient of the electrochemical
218 probe ($\text{cm}^2 \cdot \text{s}^{-1}$), $D_{25^\circ\text{C}}=6.5 \cdot 10^{-7} \text{cm}^2 \cdot \text{s}^{-1}$ and V is the scan rate ($0.1 \text{V} \cdot \text{s}^{-1}$)). Based on an average
219 peak current of $70 \mu\text{A}$, active area was found to be equal to 0.20cm^2 . This value is greatly
220 superior to usual specific surface calculated using SPCEs (a maximum of 0.07cm^2 for $\phi=3$
221 mm).

222 After the electrografting of 4-CP groups, the PGE surface was completely modified and a
223 stable and reproducible layer of COOH groups was formed. Due to the repulsive forces, the
224 electron transfer between both negatively charged redox probe and electrode surface
225 extremely decreased which resulted in the complete disappearing of both redox peaks of
226 redox probe (Fig. 2A). After the activation of the COOH groups with EDC-NHS chemistry,

227 the reversibility of the system improved, allowing the current values of the cathodic and
228 anodic peaks to increase. The aptamers were immobilized on pre-functionalized PGE surface
229 via amide coupling, which resulted in the formation of a steric barrier for the electron transfer,
230 decreasing thus the redox signal of $[\text{Fe}(\text{CN})_6]^{3-/4-}$. After incubating the aptasensor in OTA
231 solution, the aptamer underwent 3D conformational changes upon binding OTA. A decrease
232 in CV response accompanied with an increase in peak-to-peak separation confirmed the
233 interaction of aptamer sequence with OTA, forming a G-quadruplex (Badie *et al.*, 2017) that
234 blocks further the electron transfer.

235 3.1.2. Characterization of the aptasensor using EIS

236 Electrochemical impedance spectroscopy is a powerful tool for studying the electrochemical
237 behavior of modified electrode surfaces. Therefore, the stepwise development of our OTA
238 aptasensor was investigated using EIS (Fig. 2B). The impedance spectra of bare electrode
239 consisted of a semicircle portion, whose diameter corresponds to the electron transfer
240 resistance and a linear portion, which represents a diffusion-controlled process. It is well-
241 known that this behavior fits to Randles theoretical circuit. After the *in-situ* generation of 4-
242 CP diazonium salts with further carboxyl groups fixation on PGE surface, the resistance
243 significantly increased. A formed organic layer of 4-CPs acted as an electrostatic barrier
244 which repelled $[\text{Fe}(\text{CN})_6]^{3-/4-}$ anions and hindered the electron transfer between redox probe
245 and PGE surface. The resistance value increased from 30 Ω for bare electrode to 8 k Ω for 4-
246 CP modified electrode. The second modification step was the immobilization of aptamer. For
247 this purpose, the COOH groups on PGE surface were activated with EDC-NHS chemistry and
248 the aptamer was immobilized through amide coupling between NH_2 groups of the aptamer
249 sequences and pre-activated COO^- groups of the 4-CP layer. Comparing to the R_{ct} value of the
250 4-CP layer, the resistance of the aptamer-modified layer significantly decreased after the
251 aptamer immobilization. Such electrochemical behavior of modified electrode could be
252 explained by successful covering of pre-activated COO^- groups with NH_2 -terminated
253 aptamers thus, the electrostatic repulsion between COO^- groups and $[\text{Fe}(\text{CN})_6]^{3-/4-}$ anions
254 decreased. After the incubation of aptasensor in OTA solution, the R_{ct} value significantly
255 increased. In this case, the aptamer sequence underwent the conformational changes and
256 formed a G-quadruplex upon binding OTA. This formed 3D structure blocked the molecular
257 gates and did not allow ferri/ferrocyanide to freely reach the electrode surface due to the
258 electrostatic repulsion.

3.2 Optimization of aptamer immobilization

The most crucial step through the development of the aptasensor is to optimize experimental conditions for the bioreceptor immobilization onto the transducer surface, in order to achieve an aptasensing platform with a high level of stability and reproducibility. For this purpose, after obtaining a stable electrografted layer of 4-CPs, the maximum concentration of aptamer immobilized on PGE surface was optimized. Variation in the Δ_{Ratio} values was obtained in the concentration range from 0.05 μM to 1.20 μM incubating PGE in aptamer solutions for 120 min. It was observed that the saturation level of immobilized aptamer was reached in case of 0.80 μM aptamer (as illustrated in Fig. S2(A)). Moreover, different incubation times of aptamer were tested in order to achieve the maximum value of fixed aptamers. The Δ_{Ratio} values were calculated for several time intervals ranging from 30 min to 240 min. A period of 120 min as an optimized incubation time of aptamer was used (Fig. S2(B)).

Preferred place for Fig. 3

3.3 Impedimetric detection of OTA

The APT/4-CP/PGE surface, modified with specific anti-OTA aptamers, was exposed to various concentrations of OTA for 120 min in order to evaluate the analytical performances of developed aptasensors. The OTA concentration ranged from 0.1 ng/mL to 6.4 ng/mL and the PGE surface resistance was measured using EIS. In order to calculate a reliable estimation of increase in impedance, Δ_{Ratio} is calculated for all the aptasensors ($n=3$ *i.e.* different electrodes developed in triplicate).

After the incubation of aptasensors in OTA solution, a significant increase in the diameter of Nyquist circle was observed, thus, the calculated Δ_{Ratio} values was found to be directly proportional to increasing OTA concentration (Fig. 3A). A linear response of aptasensors upon binding OTA was found in the concentration range up to 1.6 ng/mL (Fig. 3B-inset). It exhibited a promising LOD of 0.1 ng.mL⁻¹, commonly based on the standard deviation of the baseline signal and a LOQ equal to 0.32 ng.mL⁻¹. According to the linear calibration curve slope, the aptasensor sensitivity is 0.33 ng.mL⁻¹.

These results suggest that the formation of aptamer/OTA complex greatly hinders the electron transfer between $[\text{Fe}(\text{CN})_6]^{3-/4-}$ and PGE surface due to aptamer rearrangement into G-

287 quadruplex structure upon recognition, which leads to the proportional increase of Rct values
288 with OTA concentration. Furthermore, OTA molecule has carboxyl and phenolic groups
289 which evidently contribute to the complex negative charges, present at the PGE surface upon
290 recognition. We believe that both electrostatic as well as steric blocking effects have
291 contributed to the increase of electron transfer resistance.

292 3.4 Aptasensor selectivity

293 Because selectivity is a critical feature of biosensing tools, control experiments were

Preferred place for Fig. 4

294 performed using OTA and its metabolite OTB as interfering analyte, since the latter belongs
295 to the same mycotoxin group. For that purpose, the 4-CP/PGEs were incubated for 120 min
296 using four different concentrations (0.4, 0.8, 1.6 and 3.2 ng.mL⁻¹) of OTA and OTB. As
297 illustrated in Fig. 4, the Δ_{Ratio} values obtained upon binding OTB did not significantly
298 increase comparing to those of OTA. These results confirmed a high level of selectivity of
299 prepared aptasensor toward OTA against low interferences of chemically similar mycotoxins.

300 3.5 Analysis of real samples

Preferred place for Table 1

301 In order to evaluate the feasibility and reliability of developed aptasensor, the beer samples
302 were spiked with OTA at three different concentrations which had been selected considering
303 the linear part of the calibration plot (0.4, 0.8 and 1.6 ng.mL⁻¹). The matrix effects were
304 reduced by 5-fold dilution of the samples in BB. As summarized in table 1, the determined
305 concentration values relatively corresponded to the spiked ones with a high level of recovery
306 percentage ($93.4 \pm 6.6\%$) which confirms the analytical capability of the aptasensor as a
307 sensing tool for OTA detection in beer industry.

308 3.6 Comparison with previous work

309 The analytical performances of our electrochemical aptasensor are compared to those of other
310 recently reported aptasensing assays using the same aptamer sequence for OTA detection.
311 This comparison is summarized in the table 2 below. It is worth mentioning that this work
312 describes the first fabrication of an OTA aptasensor based on a pencil graphite electrode,
313 which showed competitive analytical performances to SPCE-based aptasensors, widely
314 studied for mycotoxins detection as low-cost carbonaceous transducers.

315 The comparison revealed that PGE-based aptasensor offers comparable analytical
316 performances to most of the developed SPCE-based platforms. Although wider dynamic
317 ranges and lower LODs are described in some previous works, we believe that this platform
318 offers the best cost / efficiency ratio without the need to integrate nanomaterials or to label
319 aptamers as is the case of reported aptasensors in (Rivas et al., 2015) and (Catanante et al.,
320 2016) respectively. This would greatly reduce fabrication costs for a large-scale production.
321 Regarding specific beer analysis, our group reported a previous study on SPCE modification
322 with binary diazonium salt for the same detection purpose (Hayat et al., 2013). Albeit more
323 sensitive, this multi-step carbon activation seems to be time-consuming while exhibiting
324 almost the same modification yields in terms of coverage rate (96% Vs 98% in this work).

325 On the other hand, we demonstrate that using disposable PGE instead of other low-cost
326 carbonaceous electrodes for mycotoxins E-aptasensing is also practicable for real sample
327 analysis. This approach could be interesting to develop affordable affinity biosensors in any
328 laboratory equipped only with electrochemical instrumentation, since PGE are widely
329 available in every-day market with a variety of graphite compositions.

330

Preferred place for Table 2

331 **Conclusion**

332 In this project, we describe a novel label-free aptasensor based on Electrochemical Impedance
333 Spectroscopy for the direct detection of ochratoxin A, starting for the first time from low-cost
334 pencil graphite electrodes. This strategy relies on the target-induced increase in the electron
335 transfer resistance using ferro/ferricyanide as a redox probe. The EIS has been demonstrated
336 to be a sensitive method for the control of resistance changes on the electrode surface, during
337 both the stepwise fabrication process and upon target recognition. This developed tool allows
338 OTA detection at a relatively low concentration level of 0.10 ng.mL^{-1} in standard solutions
339 and 0.40 ng.mL^{-1} in beer samples. Obtained analytical performances are in good agreement
340 with standards prescribed by the EU regulation for food safety. The aptasensor showed an
341 excellent recovery rate of $93.4 \pm 6.6 \%$ in beer samples even at trace levels of the mycotoxin
342 without requiring a complex pretreatment protocol. It also showed a high level of stability and
343 reproducibility thanks to the electro-grafting method via in-situ generation of diazonium salts.
344 Interestingly, the PGE-based system showed a greater sensitivity than previously used screen-
345 printed carbon electrodes (SPCE), owing to an extended active surface area and thus a high
346 loading capacity of aptamers. Moreover, the electrochemical aptasensor has been challenged
347 against OTB as a chemically similar metabolite to prove its good selectivity toward OTA.
348 Therefore, this versatile approach opens up the path for designing highly-sensitive and cost-
349 effective aptasensors for the detection of many fungal toxins by changing simply the specific
350 aptamers.

351

352 **Acknowledgments**

353 The authors greatly acknowledge the financial support from "The Scientific and
354 Technological Research Council of Turkey (TUBITAK, 2219-2017/2). SBA is grateful for
355 financial support from European ERASMUS+ program for the mobility scholarship "EMIC",
356 as well as for the mobility grant "Bourse d'alternance" provided by the University of Tunis El
357 Manar (Tunisia).

358 **Conflict of interest**

359 The authors declare no conflict of interest.

360

361 **References**

- 362 Appell, M., Evans, K. O., Jackson, M. A., & Compton, D. L. (2018). Determination of
363 ochratoxin A in grape juice and wine using nanosponge solid phase extraction clean-up
364 and liquid chromatography with fluorescence detection. *Journal of Liquid*
365 *Chromatography & Related Technologies*, 41(15-16), 949-954.
366 <https://doi.org/10.1080/10826076.2018.1544148>
- 367 Badie, B. H., Danesh, N. M., Karimi, G., Ramezani, M., Mousavi Shaegh, S. A., Youssefi, K.,
368 Charbgoon, F., Abnous, K., & Taghdisi, S. M. (2017). Ultrasensitive detection of
369 ochratoxin A using aptasensors. *Biosensors and Bioelectronics*, 98, 168-179.
370 <https://doi.org/10.1016/j.bios.2017.06.055>
- 371 Bélanger, D., & Pinson, J. (2011). Electrografting: a powerful method for surface
372 modification. *Chemical Society Reviews*, 40(7), 3995. <https://doi.org/10.1039/c0cs00149j>
- 373 Blind, M., & Blank, M. (2015). Aptamer Selection Technology and Recent Advances.
374 *Molecular Therapy - Nucleic Acids*, 4(1), e223. <https://doi.org/10.1038/mtna.2014.74>
- 375 Bui-Klimke, T. R., & Wu, F. (2015). Ochratoxin A and Human Health Risk: A Review of the
376 Evidence. *Critical Reviews in Food Science and Nutrition*, 55(13), 1860-1869.
377 <https://doi.org/10.1080/10408398.2012.724480>
- 378 Catanante, G., Mishra, R. K., Hayat, A., & Marty, J.-L. (2016). Sensitive analytical
379 performance of folding based biosensor using methylene blue tagged aptamers. *Talanta*,
380 153, 138-144. <https://doi.org/10.1016/j.talanta.2016.03.004>
- 381 Chen, X., Huang, Y., Ma, X., Jia, F., Guo, X., & Wang, Z. (2015). Impedimetric aptamer-
382 based determination of the mold toxin fumonisin B1. *Microchimica Acta*, 182(9-10),
383 1709-1714. <https://doi.org/10.1007/s00604-015-1492-x>
- 384 Cruz-Aguado, J. A., & Penner, G. (2008). Determination of Ochratoxin A with a DNA
385 Aptamer. *Journal of Agricultural and Food Chemistry*, 56(22), 10456-10461.
386 <https://doi.org/10.1021/jf801957h>
- 387 Danesh, N. M., Bostan, H. B., Abnous, K., Ramezani, M., Youssefi, K., Taghdisi, S. M., &
388 Karimi, G. (2018). Ultrasensitive detection of aflatoxin B1 and its major metabolite
389 aflatoxin M1 using aptasensors: A review. *TrAC Trends in Analytical Chemistry*, 99,
390 117-128. <https://doi.org/10.1016/j.trac.2017.12.009>

- 391 Daniels, J. S., & Pourmand, N. (2007). Label-Free Impedance Biosensors: Opportunities and
392 Challenges. *Electroanalysis*, *19*(12), 1239-1257. <https://doi.org/10.1002/elan.200603855>
- 393 David, I. G., Popa, D.-E., & Buleandra, M. (2017). Pencil Graphite Electrodes: A Versatile
394 Tool in Electroanalysis. *Journal of Analytical Methods in Chemistry*, *2017*, 1-22.
395 <https://doi.org/10.1155/2017/1905968>
- 396 Europea, C. (2002). Assessment of dietary intake of ochratoxin A by the population of EU
397 member states. In *Reports on tasks for scientific cooperation. Reports of ...* (Numéro
398 January).
- 399 Ferapontova, E. E., Olsen, E. M., & Gothelf, K. V. (2008). An RNA Aptamer-Based
400 Electrochemical Biosensor for Detection of Theophylline in Serum. *Journal of the*
401 *American Chemical Society*, *130*(13), 4256-4258. <https://doi.org/10.1021/ja711326b>
- 402 Flajs, D., Domijan, A.-M., Ivić, D., Cvjetković, B., & Peraica, M. (2009). ELISA and HPLC
403 analysis of ochratoxin A in red wines of Croatia. *Food Control*, *20*(6), 590-592.
404 <https://doi.org/10.1016/j.foodcont.2008.08.021>
- 405 Guo, Y., Wang, X., & Sun, X. (2015). A label-free electrochemical aptasensor based on
406 electrodeposited gold nanoparticles and methylene blue for tetracycline detection.
407 *International Journal of Electrochemical Science*, *10*(4), 3668-3679.
- 408 Hayat, A., Sassolas, A., Marty, J.-L., & Radi, A.-E. (2013). Highly sensitive ochratoxin A
409 impedimetric aptasensor based on the immobilization of azido-aptamer onto
410 electrografted binary film via click chemistry. *Talanta*, *103*, 14-19.
411 <https://doi.org/10.1016/j.talanta.2012.09.048>
- 412 IARC. (1994). IARC Monographs on the Evaluation of Carcinogenic Risk to Humans, Vol.
413 56, Some Naturally Occurring Substances: Food Items and Constituents, Heterocyclic
414 Aromatic Amines and Mycotoxins. *Analytica Chimica Acta*, *294*(3), 341.
415 [https://doi.org/10.1016/0003-2670\(94\)80328-5](https://doi.org/10.1016/0003-2670(94)80328-5)
- 416 Jiang, C., Moraes Silva, S., Fan, S., Wu, Y., Alam, M. T., Liu, G., & Justin Gooding, J.
417 (2017). Aryldiazonium salt derived mixed organic layers: From surface chemistry to
418 their applications. *Journal of Electroanalytical Chemistry*, *785*, 265-278.
419 <https://doi.org/10.1016/j.jelechem.2016.11.043>
- 420 Khan, R., Ben Aissa, S., Sherazi, T., Catanante, G., Hayat, A., & Marty, J. (2019).

421 Development of an Impedimetric Aptasensor for Label Free Detection of Patulin in
422 Apple Juice. *Molecules*, 24(6), 1017. <https://doi.org/10.3390/molecules24061017>

423 Labuda, J., Brett, A. M. O., Evtugyn, G., Fojta, M., Mascini, M., Ozsoz, M., Palchetti, I.,
424 Paleček, E., & Wang, J. (2010). Electrochemical nucleic acid-based biosensors:
425 Concepts, terms, and methodology (IUPAC Technical Report). In *Pure and Applied*
426 *Chemistry* (Vol. 82, Numéro 5). <https://doi.org/10.1351/PAC-REP-09-08-16>

427 Mishra, R. K., Hayat, A., Catanante, G., Ocaña, C., & Marty, J.-L. (2015). A label free
428 aptasensor for Ochratoxin A detection in cocoa beans: An application to chocolate
429 industries. *Analytica Chimica Acta*, 889, 106-112.
430 <https://doi.org/10.1016/j.aca.2015.06.052>

431 Náchér-Mestre, J., Serrano, R., Beltrán, E., Pérez-Sánchez, J., Silva, J., Karalazos, V.,
432 Hernández, F., & Berntssen, M. H. G. (2015). Occurrence and potential transfer of
433 mycotoxins in gilthead sea bream and Atlantic salmon by use of novel alternative feed
434 ingredients. *Chemosphere*, 128, 314-320.
435 <https://doi.org/10.1016/j.chemosphere.2015.02.021>

436 Ocaña, C., & del Valle, M. (2018). Impedimetric aptasensors using nanomaterials. In
437 *Nanotechnology and Biosensors* (p. 233-267). Elsevier. [https://doi.org/10.1016/B978-0-](https://doi.org/10.1016/B978-0-12-813855-7.00008-8)
438 [12-813855-7.00008-8](https://doi.org/10.1016/B978-0-12-813855-7.00008-8)

439 Olsson, J., Börjesson, T., Lundstedt, T., & Schnürer, J. (2002). Detection and quantification of
440 ochratoxin A and deoxynivalenol in barley grains by GC-MS and electronic nose.
441 *International Journal of Food Microbiology*, 72(3), 203-214.
442 [https://doi.org/10.1016/S0168-1605\(01\)00685-7](https://doi.org/10.1016/S0168-1605(01)00685-7)

443 Patterson, D. S., & Roberts, B. A. (1979). Mycotoxins in animal feedstuffs: sensitive thin
444 layer chromatographic detection of aflatoxin, ochratoxin A, sterigmatocystin,
445 zearalenone, and T-2 toxin. *Journal - Association of Official Analytical Chemists*, 62(6),
446 1265-1267.

447 Rhouati, A., Catanante, G., Nunes, G., Hayat, A., & Marty, J. L. (2016). Label-free
448 aptasensors for the detection of mycotoxins. In *Sensors (Switzerland)* (Vol. 16, Numéro
449 12, p. 2178). Multidisciplinary Digital Publishing Institute.
450 <https://doi.org/10.3390/s16122178>

451 Rhouati, A., Hayat, A., Hernandez, D. B., Meraihi, Z., Munoz, R., & Marty, J.-L. (2013).
452 Development of an automated flow-based electrochemical aptasensor for on-line
453 detection of Ochratoxin A. *Sensors and Actuators B: Chemical*, 176, 1160-1166.
454 <https://doi.org/10.1016/j.snb.2012.09.111>

455 Rivas, L., Mayorga-Martinez, C. C., Quesada-González, D., Zamora-Gálvez, A., de la
456 Escosura-Muñiz, A., & Merkoçi, A. (2015). Label-Free Impedimetric Aptasensor for
457 Ochratoxin-A Detection Using Iridium Oxide Nanoparticles. *Analytical Chemistry*,
458 87(10), 5167-5172. <https://doi.org/10.1021/acs.analchem.5b00890>

459 Torrinha, Á., Amorim, C. G., Montenegro, M. C. B. S. M., & Araújo, A. N. (2018).
460 Biosensing based on pencil graphite electrodes. *Talanta*, 190, 235-247.
461 <https://doi.org/10.1016/j.talanta.2018.07.086>

462 Walker, R. (2002). Risk Assessment of Ochratoxin: Current Views of the European Scientific
463 Committee on Food, the Jecfa and the Codex Committee on Food Additives and
464 Contaminants. In *Mycotoxins and Food Safety* (p. 249-255). Springer, Boston, MA.
465 https://doi.org/10.1007/978-1-4615-0629-4_26

466 WHO. (2007). *WHO Technical Report Series 947 EVALUATION OF CERTAIN FOOD*
467 *ADDITIVES AND CONTAMINANTS Sixty-eighth report of the Joint FAO/WHO Expert*
468 *Committee on Food Additives Food and Agriculture Organization of the United Nations*
469 *World Health Organization*.

470 Yáñez-Sedeño, P., Campuzano, S., & Pingarrón, J. M. (2018). Integrated Affinity Biosensing
471 Platforms on Screen-Printed Electrodes Electrografted with Diazonium Salts. *Sensors*,
472 18(3), 675. <https://doi.org/10.3390/s18020675>

473 Zejli, H., Goud, K. Y., & Marty, J. L. (2018). Label free aptasensor for ochratoxin A detection
474 using polythiophene-3-carboxylic acid. *Talanta*, 185, 513-519.
475 <https://doi.org/10.1016/j.talanta.2018.03.089>

476

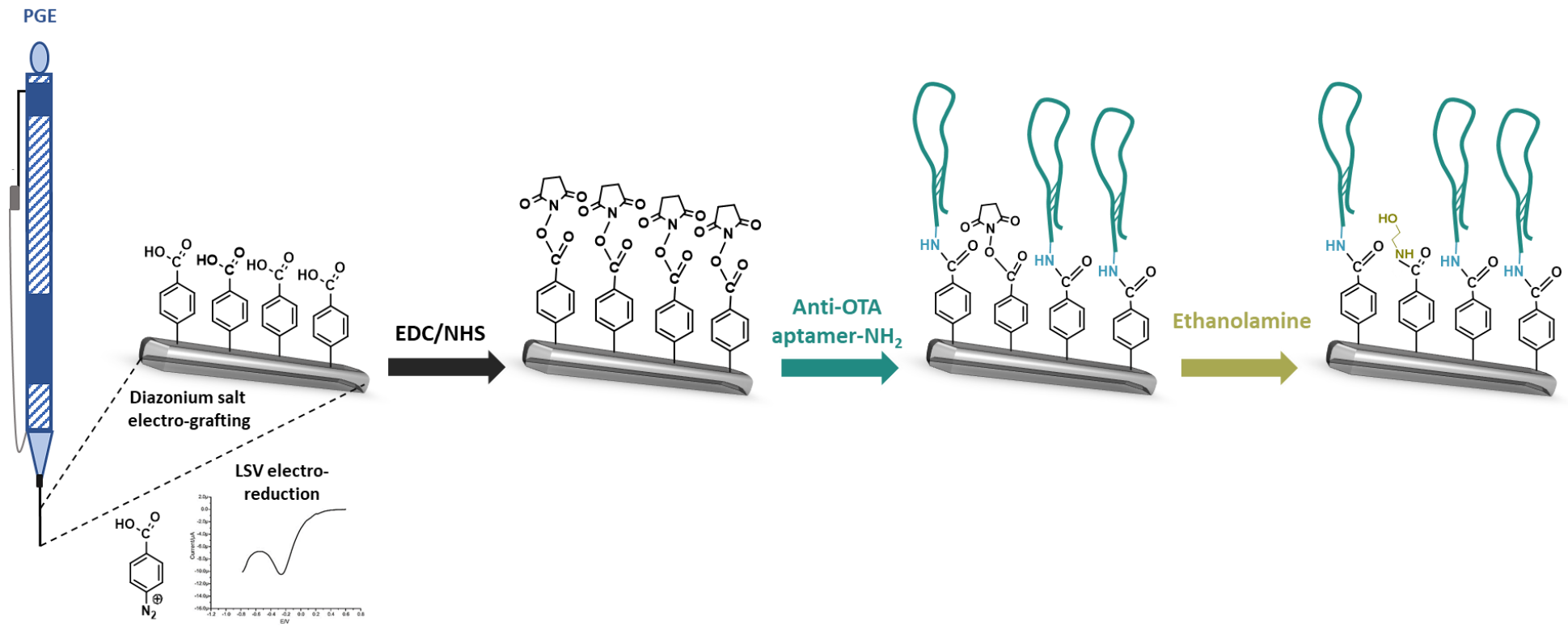


Fig. 1 Stepwise fabrication process of the PGE-based aptasensor for OTA detection

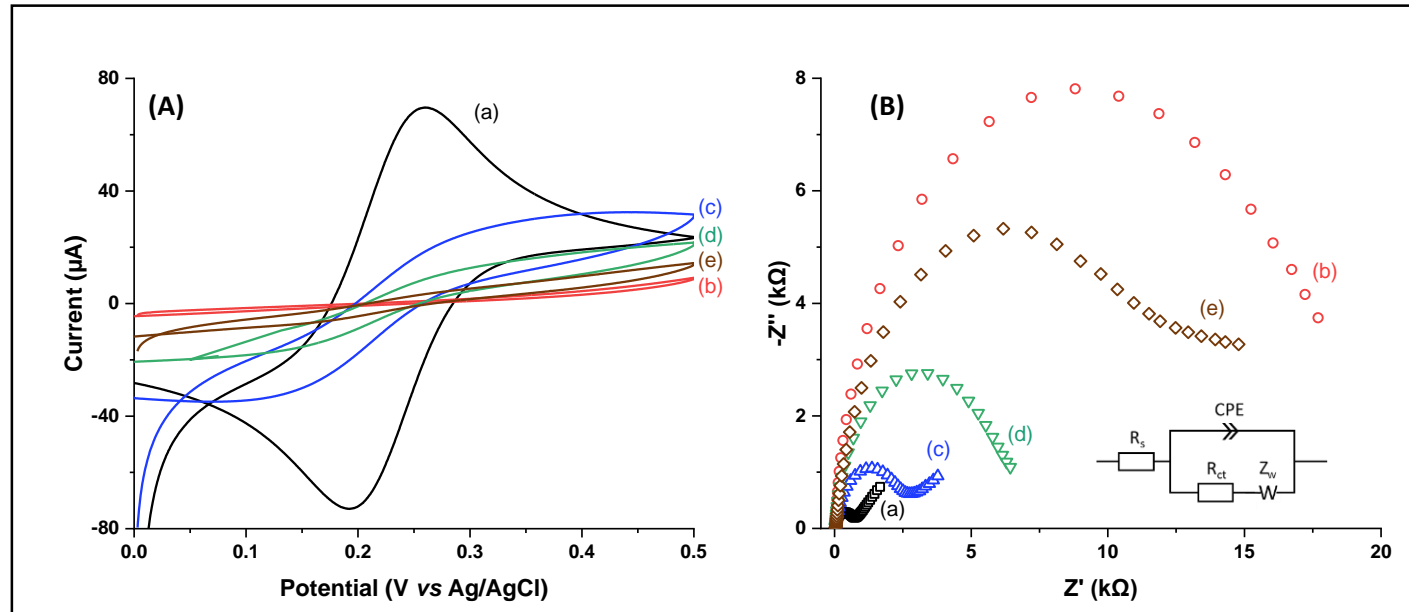


Fig. 2 (A) Cyclic voltammograms after each modification step, performed in 5 mM $[\text{Fe}(\text{CN})_6]^{3-/4-}$ at 100 $\text{mV}\cdot\text{s}^{-1}$ (B) Corresponding Nyquist plot of EIS analysis at an applied potential of 0.23 V (Vs Ag/AgCl reference electrode) using a frequency range of 10.0 kHz to 0.1 Hz and an AC amplitude of 10 mV. The inset represents the equivalent electric Randles circuit applied to fit the EIS. (a) bare PGE (b) 4-CP-modified PGE (c) activation of COOH groups on PGE (d) immobilization of 0.8 μM aptamer (e) after the incubation of aptasensor in 0.1 $\text{ng}\cdot\text{mL}^{-1}$ OTA.

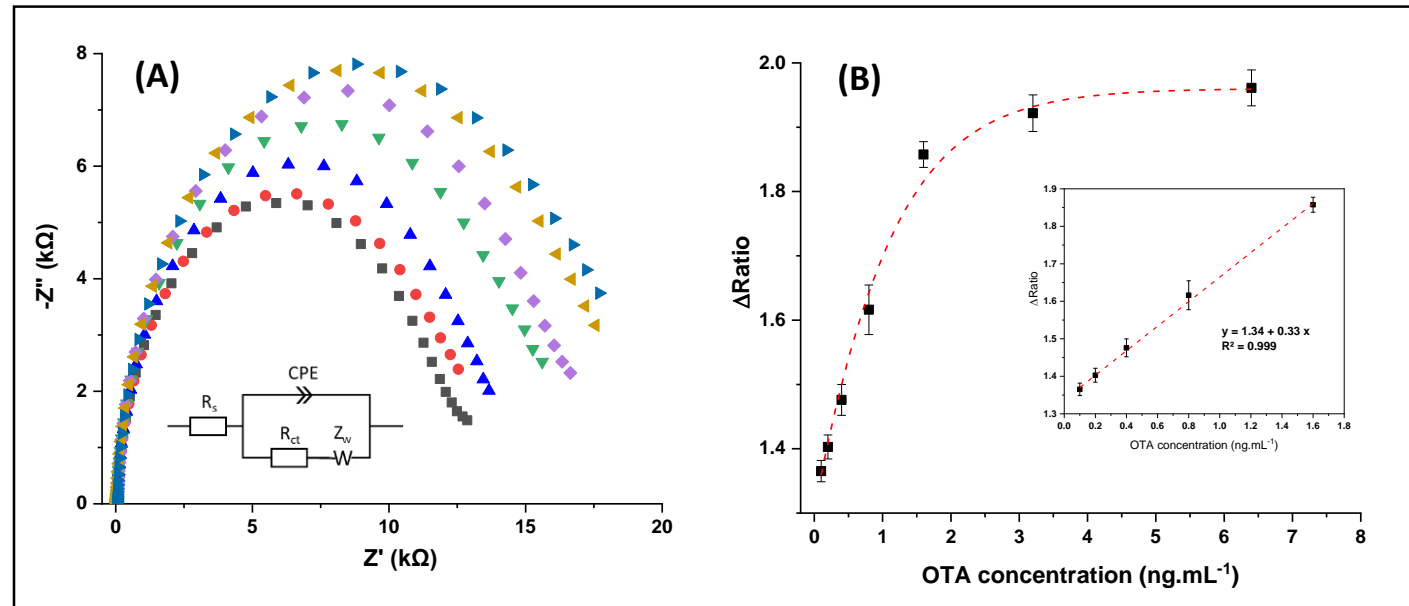


Fig. 3 (A) Nyquist plots of anti-OTA APT modified PGEs with different concentrations of OTA (ng.mL^{-1}): (a) 0.1 (b) 0.2 (c) 0.4 (d) 0.8 (e) 1.6 (f) 3.2 (g) 6.4 (B) Variations in ΔRatio values with increasing concentration of OTA from 0.1 ng.mL^{-1} to 6.4 ng/mL after the incubation time of 60 min with a linear response of aptasensor to increasing OTA concentration as an inset.

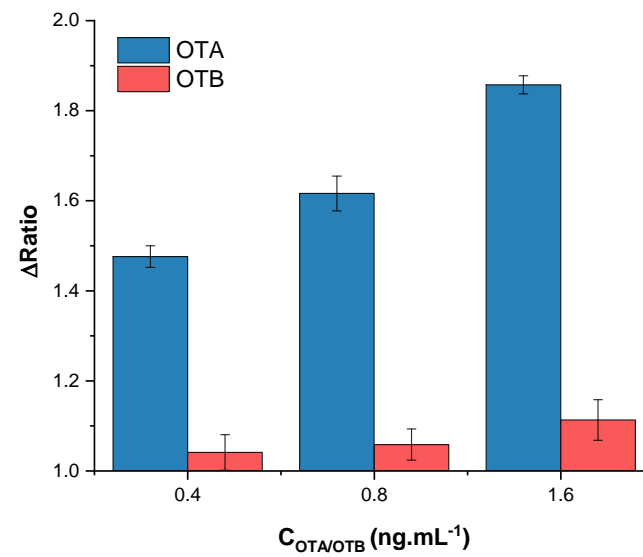


Fig. 4 Selectivity histograms presenting the calculated Δ_{Ratio} values obtained for different concentrations of OTA and OTB.

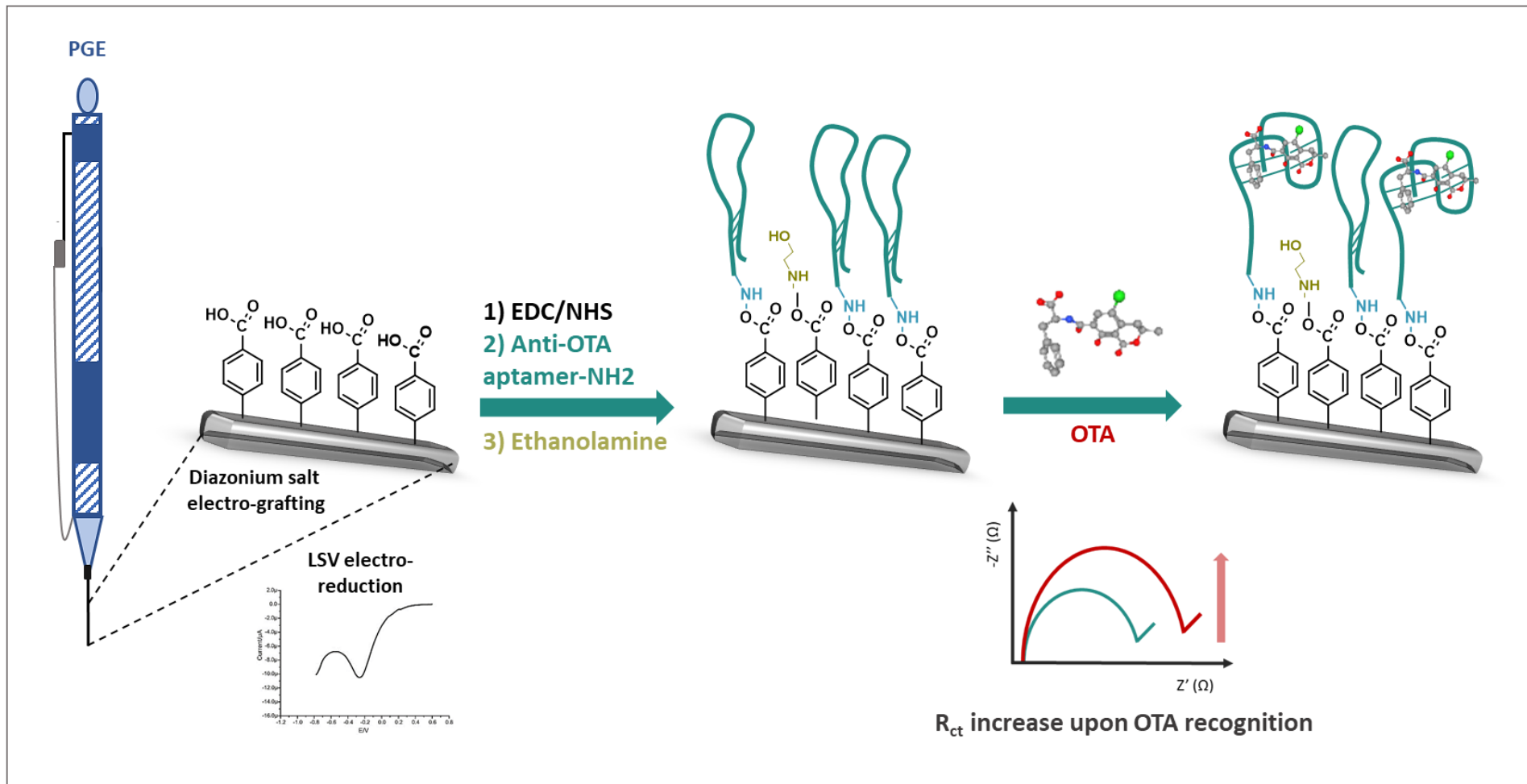
Table 1 Recoveries of OTA in spiked beer samples

Spiked OTA (ng.mL⁻¹)	Determined OTA (ng.mL⁻¹)	RSD (%)	Recovery (%)	Relative error (%)
0.4	0.37	3.49	92.10	7.90
0.8	0.75	3.95	94.12	5.88
1.6	1.50	4.95	94.03	5.96

Table 2 Comparison of the current work with some previously reported electrochemical aptasensors for OTA detection using SPCEs

Transducer	Modification	Aptamer coupling	Detection method	Dynamic range & LOD (ppb)	Real sample	Ref.
SPCE	4-((trimethylsilyl)ethynyl) benzene and p-nitrobenzene via 2-step diazonium salt electro-grafting followed by a deprotection step	Click chemistry using azido-aptamer	EIS	0.00125 - 0.5; 0.00025	Beer	(Hayat et al., 2013)
	4-ABA via diazonium salt electro-grafting	Amide coupling	EIS	0.150 - 2.5; 0.150	Cocoa beans	(Mishra et al., 2015)
	Polythionine and iridium oxide nanoparticles	Electrostatic interaction	EIS	0.004 - 40.4; 0.006	Wine	(Rivas et al., 2015)
	Hexamethylene diamine electrodeposition	Amide coupling of MB*-tagged aptamer	DPV	0.010 - 5.0; 0.010	Cocoa beans	(Catanante et al., 2016)
	Polythiophene-3-carboxylic acid	Amide coupling	EIS	0.125 – 20; 0.125	Coffee	(Zejli et al., 2018)
PGE	4-ABA via diazonium salt electro-grafting	Amide coupling	EIS	0.1 – 6.4; 0.100	Beer	<i>This work</i>

* Methylene blue



Graphical abstract : Modification of Pencil Graphite Electrode for the development of an impedimetric aptasensor for OTA detection